



Evidence for Diboson Production in the $\ell\nu$ +Heavy Flavor Jets Channel with the Full CDF II Dataset

The CDF Collaboration
URL <http://www-cdf.fnal.gov>

June 21, 2012

We present evidence for associated production of Standard Model vector bosons W and Z in a final state consistent with semileptonic plus heavy flavor quark decay ($\ell\nu + b, c$ jets). This analysis uses the full dataset collected with the CDF II detector at the Tevatron Collider at Fermilab, corresponding to an integrated luminosity of approximately 9.4 fb^{-1} . Events consistent with the signature of a high p_T charged lepton (electron or muon), large missing transverse energy and exactly two jets, of which at least one is required to contain a secondary vertex displaced from the jet origin, are selected. A multivariate discriminant based on the Support Vector Machine algorithm is used to reduce the multi-jet background contamination. Signal discrimination is based on the di-jet invariant mass and, due to the closeness of the W and the Z , the W decay into an heavy flavor jet (e.i. $W^+ \rightarrow c\bar{s}$) contributes to the signal evidence together with $Z \rightarrow b\bar{b}, c\bar{c}$.

A cross section of $\sigma_{Diboson} = 0.79 \pm 0.28 \times \sigma_{Diboson}^{SM}$ is measured for the combined diboson production. This corresponds to a significance of 3.08σ . On a second step a two dimensional discriminant based on invariant mass and a “flavor separator” Neural Network is used to measure WW and WZ/ZZ separately. The processes have been measured to have cross sections of $\sigma_{WW} = 0.45_{-0.32}^{+0.35} \times \sigma_{WW}^{SM}$ and $\sigma_{WZ/ZZ} = 1.64_{-0.77}^{+0.83} \times \sigma_{WZ/ZZ}^{SM}$, consistent with the SM prediction and corresponding to a significances of 1.78σ and 2.54σ for WW and WZ/ZZ respectively.

1 Introduction

This note describes the evidence for associated production of Standard Model (SM) vector bosons W and Z in a final state consistent with semileptonic plus heavy flavor (HF) quark decay ($\ell\nu + b, c$ jets). The search uses the full dataset collected with the CDF II detector [3] at the Tevatron Collider at Fermilab, corresponding to an integrated luminosity of approximately 9.4 fb^{-1} , and completes the results presented in [1].

The lepton plus neutrino plus two HF jets signature, although experimentally complex, is of primary importance at hadron colliders. For example, at the Tevatron, the most sensitive single channel for the SM low mass Higgs boson searches ($M_H < 140 \text{ GeV}/c^2$), is the WH associate production where the $H \rightarrow b\bar{b}$ and the W decays leptonically ($W \rightarrow \ell\nu$) [2]. Therefore the measurement of a SM resonance in the same channel is both a benchmark for the low mass Higgs boson searches, a challenging measurement, and a test of the SM predictions.

Signal candidates selection is based on reconstructed $W \rightarrow \ell\nu$ ($\ell = e, \mu$) decays produced together with two high- E_T jets consistent with a HF quark origin. The electron/muon is identified by an extended set of high- p_T charged lepton reconstruction algorithms (a total of 10) while the neutrino presence is inferred by missing transverse energy (\cancel{E}_T) in the event. At least one of the two jets should contain a reconstructed secondary decay vertex pointing to the in-flight decay of a b-hadron (“b-tagging”) [5].

The main backgrounds for the signal processes include: W +jets production (where the jets contain either tagged heavy flavor or mis-tagged light flavor), top quark production and multi-jet production (dubbed also QCD or non- W), where one jet is misidentified as a lepton. In order to increase the acceptance of our signal we use several triggers and lepton identification algorithms. To reduce the QCD background we use a multi-jet rejection algorithm based on a Support Vector Machine (SVM) discriminant exploiting the kinematic of the event.

We base our signal to background discrimination on the *invariant mass* distribution of the high- p_T jet pair entering in our selection. The secondary vertex finding algorithm reconstructs about 60% of WZ/ZZ (ZZ contribution to the $Z \rightarrow HF$ final state is about 10% with respect to WZ) decaying into heavy flavors and about 8% of the secondary vertices produced by charmed-hadrons coming from WW . On a following step, a flavor-separator Neural Network [9] (KIT-NN) exploiting more of the secondary vertex properties, is used to separate WW from WZ/ZZ contribution.

2 Data Sample & Event Selection

This analysis uses the full CDF II dataset: collected between March 2002 and September 2011. After data quality requirements, it corresponds to an integrated luminosity of 9.4 fb^{-1} . We select events consistent with the signature of a W boson leptonic decay, large missing transverse energy and exactly two energetic jets. We accept tight charged lepton candidates, loose muon candidates (a total of five different algorithms) and isolated tracks; by construction these lepton categories are orthogonal to each other. In the following, sometimes, we refer to these categories of events as:

- CEM: central tight electrons;

- PHX: forward (or “Plug”) tight electrons;
- CMUP and CMX: central tight muons;
- EMC (Extended Muon Categories): loose muons plus isolated track lepton candidates [10].

Selection starts online with an ensemble of different triggers. Tight central electrons (muons) are collected by requiring a lepton with $E_T(p_T) > 18$ GeV (GeV/c). Tight forward electrons are collected by a joint requirement of $\cancel{E}_T > 15$ GeV and electromagnetic calorimeter clusters of 20 GeV in the region $1.1 < |\eta| < 2.4$.

Data containing loose leptons and isolated tracks are gathered using a set of triggers based on missing transverse energy (\cancel{E}_T) and jet information.

Offline the selection of a sample of W +jets events is performed by requiring, in each event, two leptons (one isolated and charged and a neutrino) and two jets. Therefore we ask for $\cancel{E}_T > 15$ GeV and a single, isolated electron (muon) with $E_T(p_T) > 20$ GeV(GeV/c) in the central ($|\eta_{Det}| < 1.1$) or forward ($1.2 < |\eta_{Det}| < 2.0$) part of the detector. Jets are reconstructed with a cone algorithm of radius $R = 0.4$. We require exactly two jets with $|\eta_{Det}| < 2.0$ and $E_T^{corr} > 20$ GeV, after jet energy corrections for detector effects [4].

Multi-jet (non- W) background is further suppressed with the use of a multivariate technique (see Section 2.1).

As we are looking for events in which W or Z bosons decay into heavy flavour, we further require that at least one of the two jets is originating from a HF-hadron quark tagged by the Secondary Vertex tagger algorithm [5] (SecVtx).

2.1 Suppression of Multi-jet Background

A fake W -boson-like signature can be generated when one jet fakes a high p_T lepton and \cancel{E}_T comes from jet energy mis-measurement. We developed a method to suppress the multi-jet background using a multivariate technique based on the Support Vector Machine algorithm (SVM) [6]. We developed a software package, based on the LibSVM [7] library, able to perform algorithm training, variable ranking, signal discrimination and robustness test. We trained two discriminants, one for the central electron sample and one for the forward electron samples¹. The signal model is based on the Alpgen [8] $W \rightarrow e\nu + 2, 3$ parton MC while data driven multi-jet models have been used for the background. Signal-background separation has been obtained exploiting kinematic variables.

In the previous analysis [1], the SVM was used as a binary classifier between W +jet *vs* multi-jet events, while, this time, the continuous output distribution of the discriminant

¹The multi-jet contamination is from two to three times higher in the forward reconstructed electrons with respect to the central electron selection.

is used both in the selection and in the estimate of the multi-jet contamination. As explained later in Section 3, the multi-jet contamination is unknown a-priori and should be derived with a fit on a sensitive variable. The newly trained SVMs demonstrated a good separation power between multi-jet and W +jets events and sensitivity to the final multi-jet contamination in the signal region. Figure 1 shows the fitted SVM output distributions used to evaluate QCD contribution for the CEM, PHX, CMUP and CMX categories.

The SVM trained on the central electron sample was successfully used also on all the other central selected events (tight muons, loose muons and isolated tracks) because the machine is based only on the kinematic properties of W +jets and multi-jet events.

Overall we achieve a large reduction of the multi-jet contamination in all the lepton categories (with a fraction of QCD events ranging from $\approx 15\%$ for PHX to negligible amounts for tight muons), maintaining a very high efficiency on the signature $p\bar{p} \rightarrow \ell\nu + jj$ ($\epsilon_{W+jets} \approx 95\%$).

3 Backgrounds

Since our final state has the signature of a charged lepton, \cancel{E}_T and two jets (a W boson and jets signature), the following background sources are considered:

Non-W/Multi-jet : a W -boson-like signature is generated when one jet fakes a high p_T lepton and \cancel{E}_T is generated through jet energy mis-measurement.

W + Mistags: this background occurs when one or more light flavor jets produced in association with a W boson are mistakenly identified as a heavy flavor jet by the b -tagging algorithm. Mistags are generated because of the finite resolution of the tracking detectors, material interactions, or from long-lived light flavor hadrons (Λ and K_s) which produce real displaced vertices. The mistag probability of a generic jet is measured in a multi-jet control sample and parametrized as a function of six significant variables (“mistag matrix”).

W + Heavy Flavor: these processes ($W+b\bar{b}$, $W+c\bar{c}$ and $W+c$) involve the production of heavy flavor quarks in association with a W boson.

Other Electroweak Backgrounds: additional small but non-negligible background contributions come from single top quark and top quark pair production, Z boson + jets production.

We determine the amount of selected W +jets events for each lepton category by fitting the SVM distribution of the pretag data control sample (see Figure 1): for top and electroweak components the MC templates are normalized to the theoretical expectation while for W +jets and non- W the normalization is free to float in the likelihood fit used.

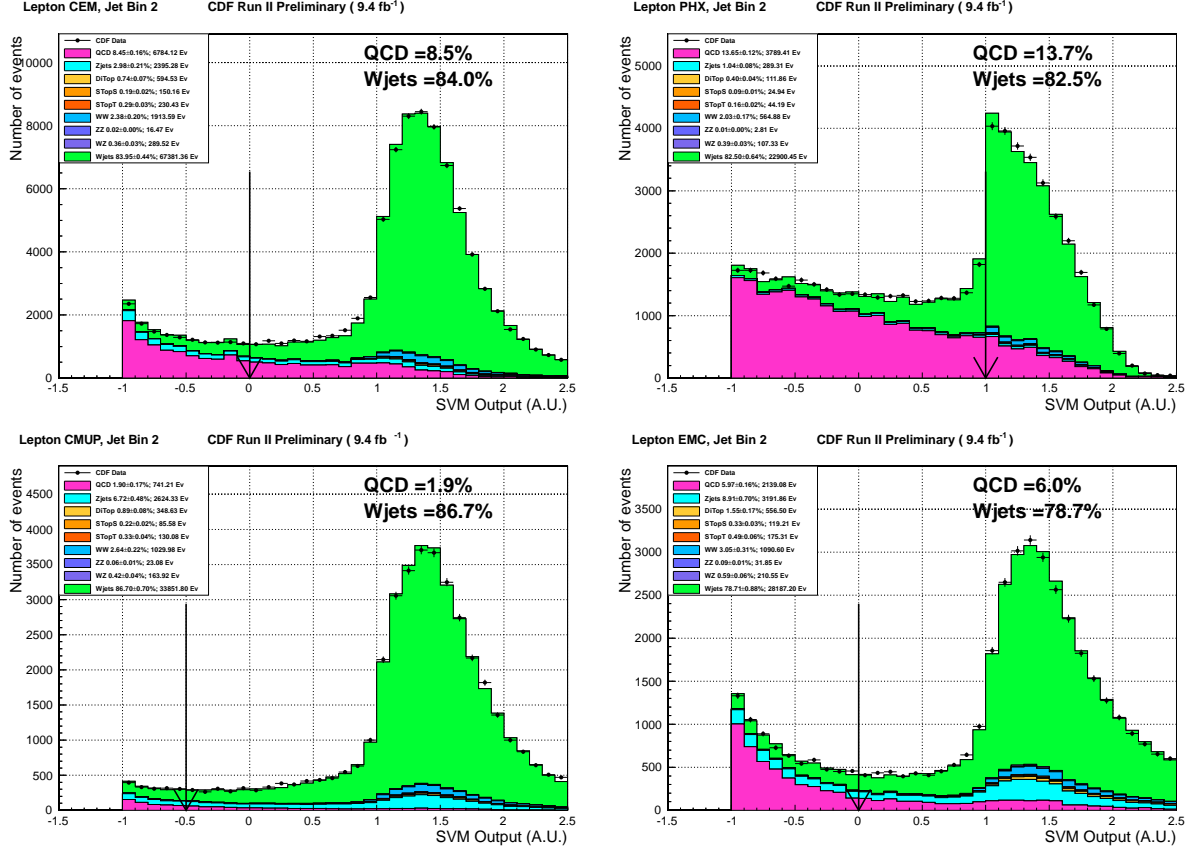


Figure 1: W +jets (green) and QCD (pink) fraction estimates for the Pretag control region derived from a fit on the SVM output distribution. The figure shows (left to right and top to bottom) CEM, PHX, CMUP and EMC charged lepton categories. The reported percentage refers to the fractions of the components beyond the signal selection cut pointed by arrows.

The following samples are used to produce the non- W templates:

- “anti-electrons” CEM specific;
- “anti-electrons” PHX specific;
- non-isolated (isolation > 0.2) tight muons for the central tight muons fakes;
- non-isolated (isolation > 0.2) loose muons to mimic the EMC categories.

The anti-electron non- W templates are built by inverting 2 out of 5 electron shower identification variables; this selection criteria can bias the QCD model. In order to

improve the model, we apply a correction to the E_T of the CEM anti-electron events based on the calorimeter response to the anti-electron candidate.

The b -tagged W + heavy flavor (HF) component is extracted from the total W +jets pretag sample: the total W +jets is composed by a large set of Alpgen+Pythia [11] Monte Carlo weighted by their LO production cross section, the HF fractions are then extracted and scaled for the NLO contribution and b -tagging algorithm efficiency.

We estimate the normalization of W + mistags background by applying the mistag matrix to the pretag data after subtracting the non- W , top, diboson, Z +jets and W + HF contributions. We model the W + mistag kinematics and shapes using W + light flavor Monte Carlo events weighting each event for the mistag probability.

The top quark and other electroweak backgrounds are normalized directly to their theoretical cross sections, calculated at next-to-leading order.

Finally the residual tagged non- W component is fitted to the data together with a template of all the other backgrounds: the two normalizations are free to float and the multi-jet one is extracted. More details on the background estimate can be found in Ref [9].

Tables 1 and 2 summarize the number of observed and expected events in the W +2 jets sample, for all lepton categories, with one b -tag and with two b -tags, respectively.

4 $M_{inv}(jet1, jet2)$ distribution

Signal discrimination is based on the invariant mass of the two jets ($M_{inv}(jet1, jet2)$) for double tag events and on the bi-dimensional distribution of $M_{Inv}(jet1, jet2)$ against the KIT-NN output for the single tag events. The KIT-NN output, ranging from -1 to 1, is divided in four equal size bins: the right-most is the most enriched in b -like secondary vertices, while the others have variable composition of b -like, c -like and mistag-like jets. The final result is based on a total of eight different channels: 4 lepton sub-samples (CEM, PHX, Tight Muons, EMC) \times 2 b -tag prescriptions (1 tag with KIT-NN and 2 tags). The $M_{inv}(jet1, jet2)$ distribution combining all of the lepton categories for the single-tag channel is shown in Figure 2, integrated across all the KIT-NN values. Figure 3 shows the single-tag $M_{inv}(jet1, jet2)$ distribution for the b -enriched KIT-NN region (KIT-NN > 0.5, right plot) and the $M_{inv}(jet1, jet2)$ distribution corresponding to the low score KIT-NN bins (KIT-NN < 0.5, left plot). Finally, the $M_{inv}(jet1, jet2)$ distribution for double-tagged events is shown in Figure 4. $M_{inv}(jet1, jet2)$ plots shown here are normalized to the values returned by the final fit, with a full treatment of the correlated systematic effects (see next paragraph for a complete description).

Table 1: Summary of observed and expected events with one secondary vertex tag (SecVtx), in the W+2 jets sample, in 9.4 fb^{-1} of data in the different lepton categories.

Chennel	CEM	CMUP	CMX	EMC	PHX
Pretag Data	80263	39045	22465	35810	27759
Zjets	55.53 ± 4.73	65.3 ± 5.73	37.14 ± 3.28	104.18 ± 10.8	7.76 ± 0.67
$t\bar{t}$	237.55 ± 23.3	139.68 ± 13.8	62.22 ± 6.14	228.58 ± 25.6	46.93 ± 4.59
Single Top s	64.23 ± 5.88	36.42 ± 3.35	16.11 ± 1.49	51.68 ± 5.48	11.08 ± 1.02
Single Top t	84.95 ± 9.99	47.75 ± 5.64	22.5 ± 2.66	66.22 ± 8.56	16.86 ± 1.98
WW	84.35 ± 11.8	43.7 ± 6.17	23.68 ± 3.35	53.11 ± 8	25.05 ± 3.54
ZZ	1.85 ± 0.19	2.45 ± 0.25	1.37 ± 0.14	3.45 ± 0.39	0.21 ± 0.02
WZ	29.2 ± 2.95	16 ± 1.66	9.21 ± 0.94	20.54 ± 2.39	12.32 ± 1.22
W+ $b\bar{b}$	858.71 ± 258	428.58 ± 129	238.99 ± 71.9	409.97 ± 123	263.08 ± 79.1
W+ $c\bar{c}$	441.77 ± 134	212.98 ± 64.8	120.26 ± 36.6	214 ± 65	145.08 ± 44.1
W+cj	342.86 ± 104	171.77 ± 52.2	93.01 ± 28.3	143.47 ± 43.6	96.42 ± 29.3
Mistags	809.01 ± 87.1	408.74 ± 43.3	230.75 ± 24.7	463.65 ± 53.5	302.78 ± 32.2
Non-W	302.69 ± 121	58.75 ± 23.5	27.96 ± 11.2	106.35 ± 42.5	205.06 ± 82
Prediction	3312.68 ± 521	1632.11 ± 253	883.21 ± 140	1865.2 ± 248	1132.63 ± 176
Observed	3115	1577	830	1705	1073
Dibosons	115.39 ± 13	62.15 ± 6.87	34.26 ± 3.75	77.09 ± 9.35	37.57 ± 4.05

4.1 Cross Section Measurement and Statistical Analysis

The process diboson $\rightarrow \ell\nu + HF$ was never observed before in a single analysis. In order to measure the diboson production cross section, a maximum likelihood Bayesian marginalization technique [12] is applied to the $M_{inv}(jet1, jet2)$ vs $KIT - NN$ distribution for 1-tag samples and $M_{inv}(jet1, jet2)$ for 2 tags samples. The following systematic uncertainties (for background and signal) are taken into account as normalization nuisance parameters (min-max variation is in parenthesis): JES (1–14%), Alpgen Q^2 (1–17%), b-tagging efficiency scale factor ² (3–24%), lepton identification and trigger efficiencies (1–4%), multi-jet background normalization (40%), NLO scaling of W+heavy flavor production (30%), ISR/FSR (1-4% for signal only) and mistag uncertainty (12–25%). In addition JES, Q^2 and KIT-NN c /light-flavor parametrization, are taken as shape systematics as well, where the interpolated shape variation is used as nuisance parameter. All the nuisance parameters are integrated in the fit to improve the sensitivity.

²Efficiency for c -matched jets in MC have never been measured directly, although the sources of HF-tagging uncertainties are supposed to be the same as for b -matched jets. A conservative prescription is to double the systematic error with respect to the b -jet standard.

Table 2: Summary of observed and expected events with two secondary vertex tags (SecVtx), in the W+2 jets sample, in 9.4 fb^{-1} of data in the different lepton categories.

Chennel	CEM	CMUP	CMX	EMC	PHX
Pretag Data	80263	39045	22465	35810	27759
Zjets	1.43 ± 0.13	2.84 ± 0.27	1.41 ± 0.13	4.6 ± 0.5	0.27 ± 0.02
$t\bar{t}$	48.21 ± 6.99	27.31 ± 3.98	12.37 ± 1.8	44.89 ± 6.95	9.91 ± 1.44
Single Top s	16.89 ± 2.36	9.68 ± 1.36	4.17 ± 0.58	13.72 ± 2.05	2.87 ± 0.4
Single Top t	5.07 ± 0.81	2.85 ± 0.46	1.34 ± 0.22	4.16 ± 0.71	1.13 ± 0.18
WW	0.72 ± 0.19	0.35 ± 0.09	0.2 ± 0.05	0.49 ± 0.13	0.18 ± 0.05
ZZ	0.26 ± 0.04	0.46 ± 0.06	0.29 ± 0.04	0.63 ± 0.1	0.03 ± 0
WZ	5.28 ± 0.75	2.52 ± 0.36	1.67 ± 0.24	3.52 ± 0.54	2.6 ± 0.37
$W+b\bar{b}$	114.7 ± 35.1	59.06 ± 18.1	29.49 ± 9.04	60.71 ± 18.6	33.92 ± 10.4
$W+c\bar{c}$	6.68 ± 2.1	3.41 ± 1.08	1.63 ± 0.51	4 ± 1.25	2.16 ± 0.68
$W+cj$	5.18 ± 1.63	2.75 ± 0.87	1.26 ± 0.4	2.69 ± 0.84	1.43 ± 0.45
Mistags	4.53 ± 0.94	2.35 ± 0.48	1.28 ± 0.27	2.98 ± 0.66	1.7 ± 0.36
Non-W	5.58 ± 2.23	4.31 ± 1.73	0 ± 0.5	0 ± 0.5	6.79 ± 2.72
Prediction	214.53 ± 40.5	117.92 ± 21.1	55.11 ± 10.4	142.38 ± 23.3	62.99 ± 12.1
Observed	175	92	49	126	62
Dibosons	6.26 ± 0.79	3.34 ± 0.4	2.15 ± 0.26	4.64 ± 0.61	2.8 ± 0.38

The diboson signal cross section is first measured leaving the production cross section of the WW and WZ/ZZ component constrained to the SM ratio, obtaining a cross section of $\sigma_{Diboson}^{Obs} = 0.79 \pm 0.28 \times \sigma_{Diboson}^{SM}$. The resulting Bayesian posterior distribution is shown in Figure 5 together with the 68% and 95% confidence intervals.

To compute the significance of the measurement we performed a hypothesis test comparing data to the Null hypotheses (H_0): H_0 assumes all the predicted background processes except diboson production. Pseudo-experiments (PEs) are extracted from H_0 distribution. Figure 6 shows the possible outcomes of many cross section measurements in a background-only and in a background+signal hypothesis. The number of times a background fluctuation produces cross section measurement greater than $\sigma_{Diboson}^{Obs} = 0.79 \times \sigma_{Diboson}^{SM}$ gives a p -value of 0.0209. The result is evidence for diboson production in the $\ell\nu + HF$ final state with a significance of 3.08σ .

On a successive step we exploited the KIT-NN separation power of c versus b jets to have a separate measurement of WW against WZ/ZZ processes³. We iterated the cross section measurement procedure but, this time, σ_{WW} and $\sigma_{WZ/ZZ}$ are left free to float independently (i.e. not constrained to the SM ratio). Figure 7 shows the measured

³the small ZZ contribution to our signal is impossible to distinguish from the WZ one.

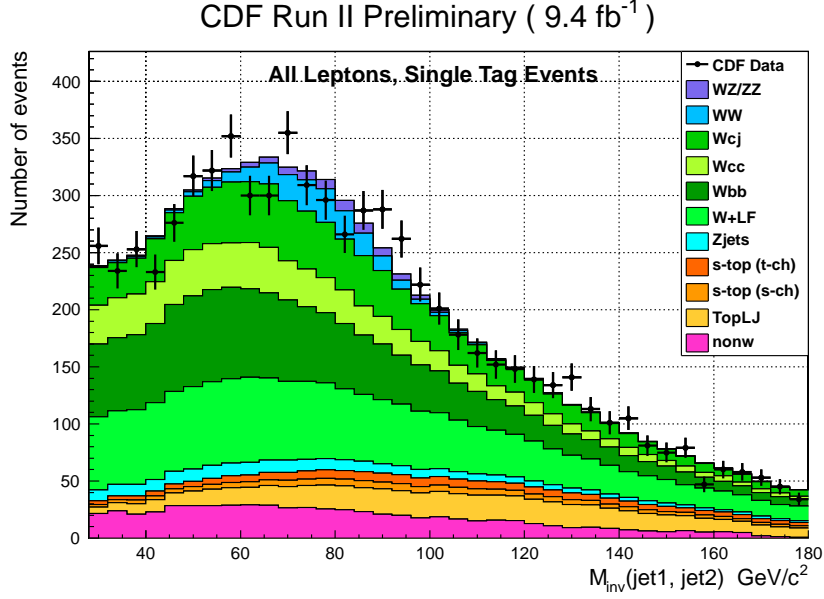


Figure 2: $M_{Inv}(jet1, jet2)$ distribution for the 1 SecVtx tag candidates where all the lepton categories have been added together (CEM+PHX+CMUP+CMX+EMC combined). The best fit values for the rate and shape of the backgrounds are used in the figure.

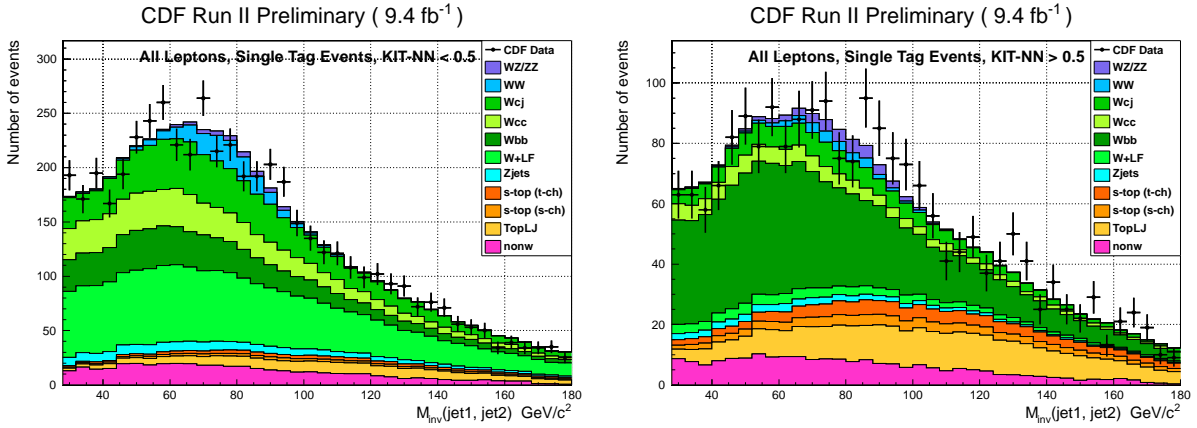


Figure 3: $M_{Inv}(jet1, jet2)$ distribution for the 1 SecVtx tag candidates separate depending on the KIT-NN score on the tagged jet: on left, in case $KIT-NN < 0.5$, on the right, in case $KIT-NN > 0.5$. All the lepton categories have been added together (CEM+PHX+CMUP+CMX+EMC combined) and the best fit values for the rate and shape of the backgrounds are used in the figure.

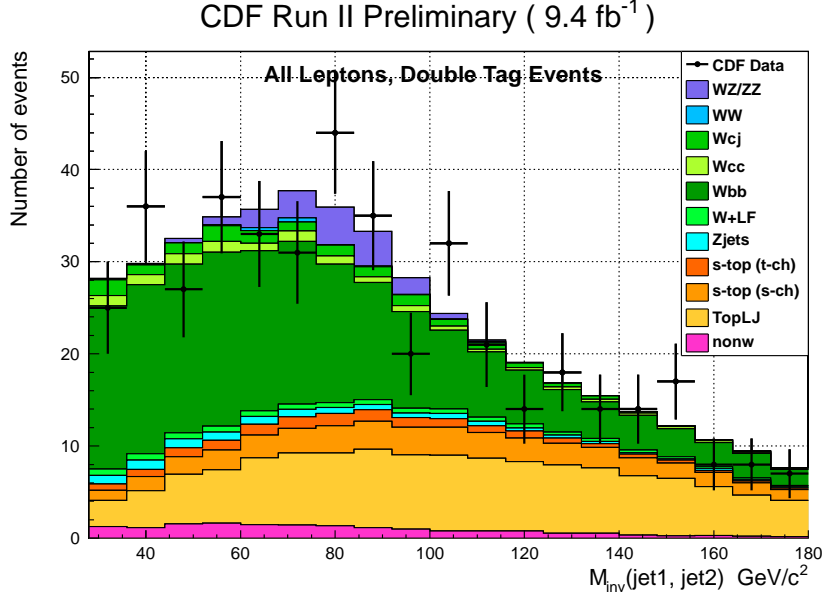


Figure 4: $M_{Inv}(jet1, jet2)$ distribution for the 2 Sec Vtx tag candidates where all the lepton categories have been added together (CEM+PHX+CMUP+CMX+EMC combined). The best fit values for the rate and shape of the backgrounds are used in the figure.

Bayesian posterior distribution scaled to SM expectation: the maximum value gives the measured cross sections of $\sigma_{WW}^{Obs,2D} = 0.50 \times \sigma_{WW}^{SM}$ and $\sigma_{WZ/ZZ}^{Obs,2D} = 1.56 \times \sigma_{WZ/ZZ}^{SM}$ with integration contours at 1, 2 and 3 σ levels.

To analyze WW and WZ/ZZ channels separately, we projected the two-dimensional Bayesian posterior on the σ_{WW} and the $\sigma_{WZ/ZZ}$ axes, in this way we consider, one at the time, the two processes as background. For both WW and WZ/ZZ we re-computed maximum values and confidence intervals, results are shown in Figures 8. The measured cross sections are: $\sigma_{WW}^{Obs} = 0.45^{+0.35}_{-0.32} \times \sigma_{WW}^{SM}$ and $\sigma_{WZ/ZZ}^{Obs} = 1.64^{+0.83}_{-0.78} \times \sigma_{WZ/ZZ}^{SM}$.

WW and WZ/ZZ significances have been evaluated in a similar way: we generated PEs with *null hypothesis* on both WW and WZ/ZZ signals. Then, the cross sections measured on the σ_{WW} vs $\sigma_{WZ/ZZ}$ plane have been projected along the axes and compared with σ_{WZ}^{Obs} and $\sigma_{WZ/ZZ}^{Obs}$. The result of the p -value estimates are reported in Figure 9, we obtain: $p\text{-value}_{WW} = 0.074565$ and $p\text{-value}_{WZ/ZZ} = 0.011145$. They correspond to a significance of 1.78σ and 2.54σ for WW and WZ/ZZ respectively. The upward fluctuation of $\sigma_{WZ/ZZ}$ is consistent with the measurement obtained in the latest WH search by CDF [13] although with a completely different tagging strategy and final discriminant variable.

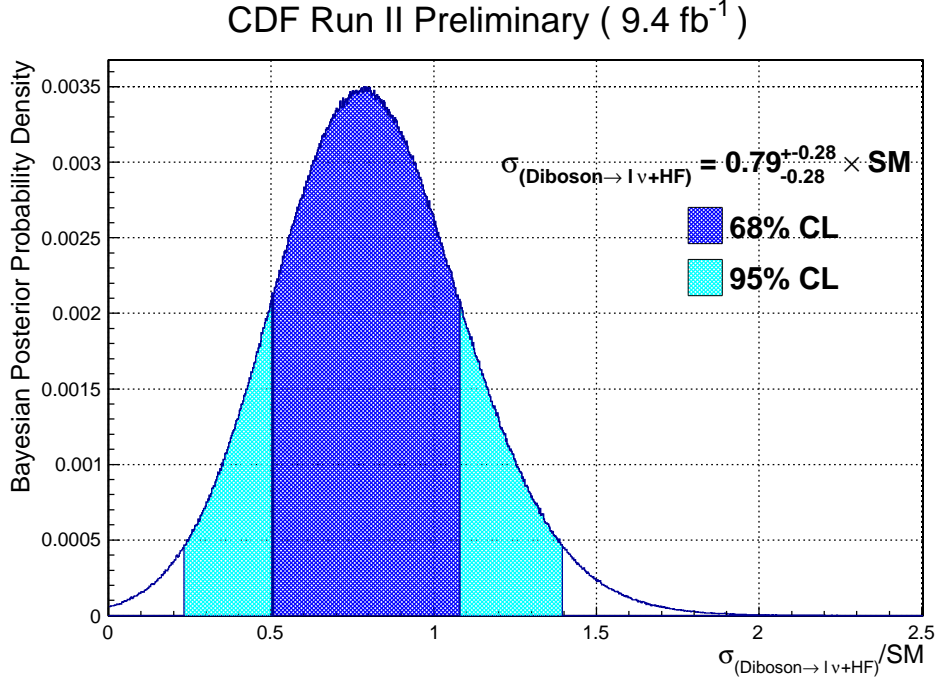


Figure 5: *The Bayesian posterior, marginalized over nuisance parameters, is shown. The maximum value is the central value of the cross-section. The blue and azure areas represent the smallest intervals enclosing 68% and 95%, of the posterior integrals, respectively.*

5 Conclusions

We analyzed the full CDF II dataset, corresponding to 9.4 fb⁻¹ of data, looking for the $\text{Diboson} \rightarrow l\nu + \text{HF}$ signal in the $W + 2$ jets exclusive sample. We found an excess over the background-only hypothesis in the $M_{inv}(\text{jet1}, \text{jet2})$ distribution looking at the double tagged and single tagged events: the result is consistent with evidence (3.08σ) for diboson associate production with one vector boson decaying semileptonically and the other decaying into HF jets ($W \rightarrow cs$ and $Z \rightarrow c\bar{c}, b\bar{b}$). The measured cross section is $\sigma_{\text{Diboson}} = 0.79 \pm 0.28 \times \sigma_{\text{Diboson}}^{\text{SM}}$.

With the help of a flavor-separator NN we measured WW and WZ/ZZ processes separately and we obtained the following measurements: $\sigma_{WW} = 0.45^{+0.35}_{-0.32} \times \sigma_{WW}^{\text{SM}}$ and $\sigma_{WZ/ZZ} = 1.64^{+0.83}_{-0.77} \times \sigma_{WZ/ZZ}^{\text{SM}}$ with significances of 1.78σ and 2.54σ for WW and WZ/ZZ respectively. The results are constant with the SM predictions for diboson associate production and decay in the $l\nu + \text{HF}$ channel.

CDF Run II Preliminary (9.4 fb⁻¹)

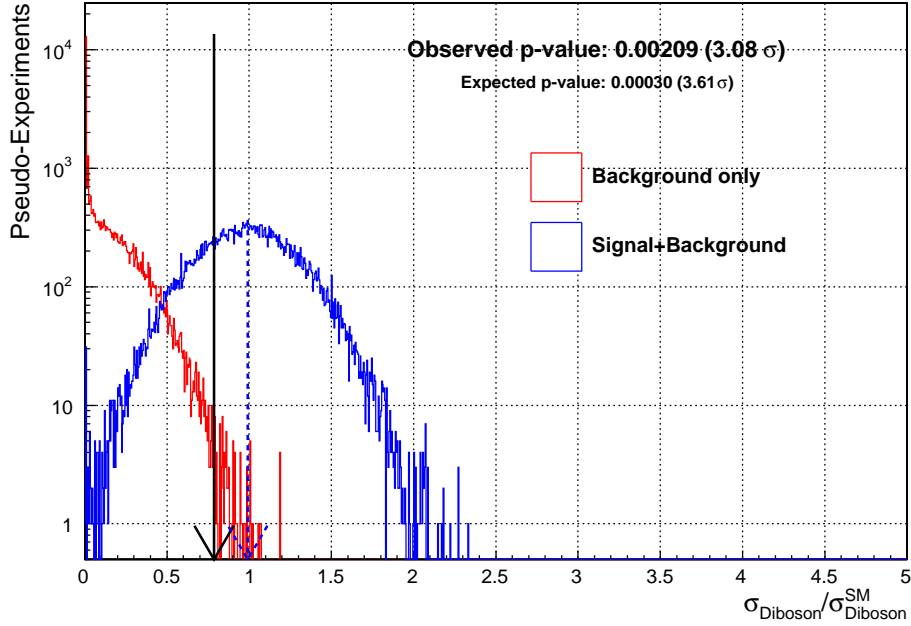


Figure 6: Possible outcomes of many diboson cross section measurements on Pseudo Experiments (PEs) generated in a background-only and in a background+signal hypothesis. The p -value for $\sigma_{Diboson}^{Obs} = 0.79 \times \sigma_{Diboson}^{SM}$ is 0.0209, corresponding to a significance of 3.08σ .

Acknowledgments

We thank the Fermilab staff and the technical staffs of the participating institutions for their vital contributions. This work was supported by the U.S. Department of Energy and National Science Foundation; the Italian Istituto Nazionale di Fisica Nucleare; the Ministry of Education, Culture, Sports, Science and Technology of Japan; the Natural Sciences and Engineering Research Council of Canada; the National Science Council of the Republic of China; the Swiss National Science Foundation; the A.P. Sloan Foundation; the Bundesministerium fuer Bildung und Forschung, Germany; the Korean Science and Engineering Foundation and the Korean Research Foundation; the Particle Physics and Astronomy Research Council and the Royal Society, UK; the Russian Foundation for Basic Research; the Comision Interministerial de Ciencia y Tecnologia, Spain; and in part by the European Community's Human Potential Programme under contract HPRN-CT-20002, the Slovak R and D agency and the Academy of Finland.

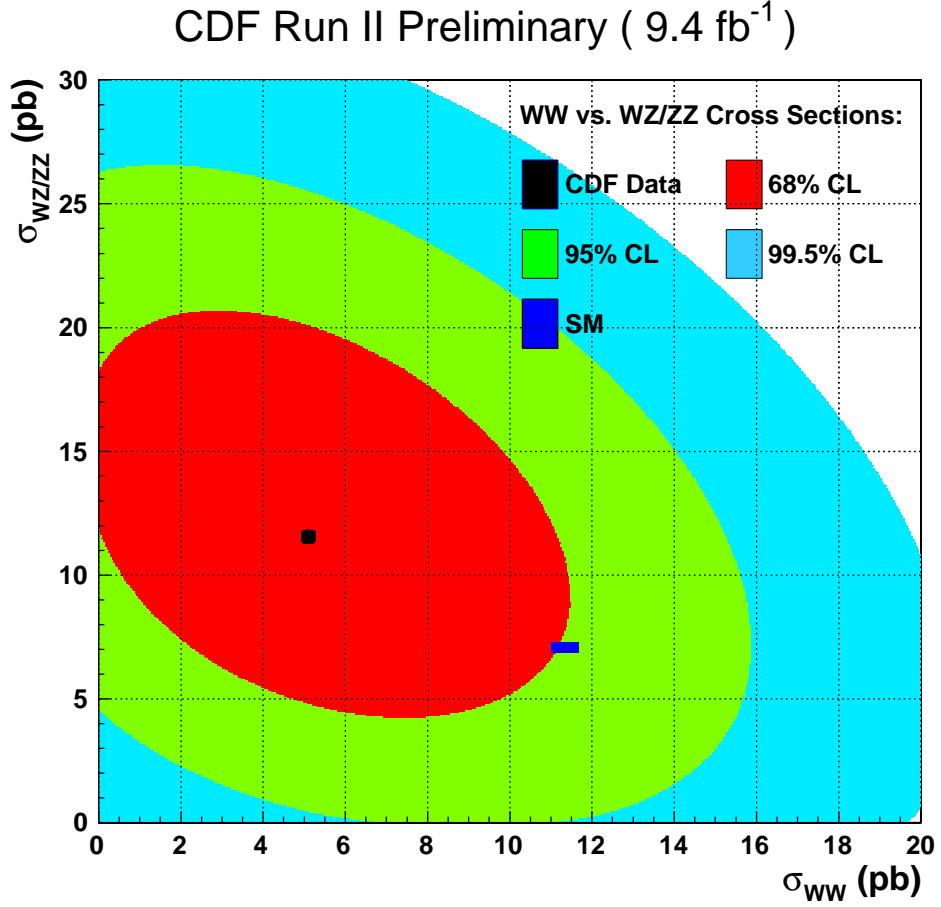


Figure 7: *The Bayesian posterior, marginalized over nuisance parameters and scaled to SM expectation, is shown in the plane σ_{WW} vs $\sigma_{WZ/ZZ}$. The measured cross sections correspond to the maximum value of $\sigma_{WW}^{Obs,2D} = 0.50 \times \sigma_{WW}^{SM}$ and $\sigma_{WZ/ZZ}^{Obs,2D} = 1.56 \times \sigma_{WZ/ZZ}^{SM}$. The red, blue and azure areas represent the smallest intervals enclosing 68%, 95% and 99% of the posterior integrals, respectively.*

References

- [1] G. Chiarelli, S. Leone, F. Sforza, “Search for $WW/WZ \rightarrow \ell\nu + HF$ just vector boson production in 7.5 fb-1 of CDF data”, CDF Public Note 10703 (2011).
- [2] T. Aaltonen et al. (CDF Collaboration), Accepted by PRD, arXiv:1112.4358.
- [3] F. Abe, et al., Nucl. Instrum. Methods Phys. Res. A **271**, 387 (1988); D. Amidei, et

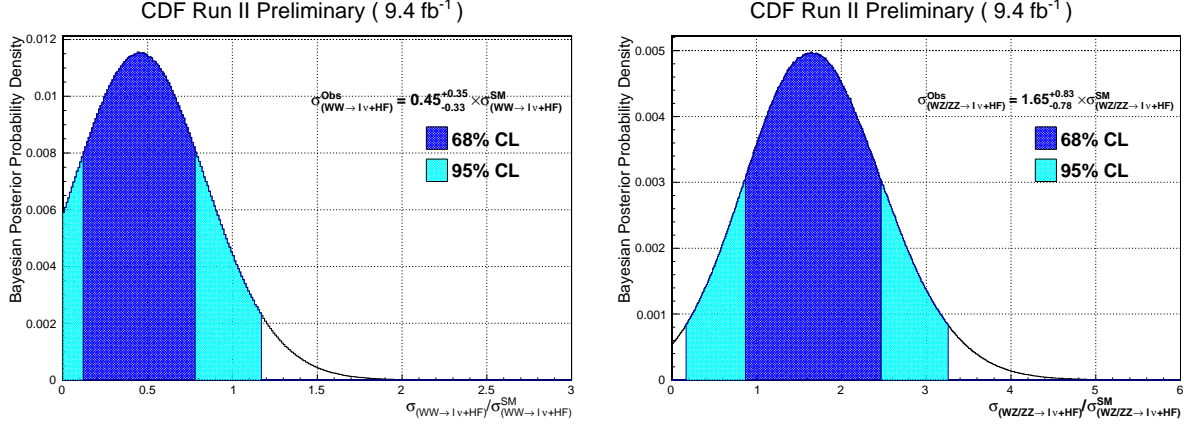


Figure 8: The Bayesian posterior, function of σ_{WW} and $\sigma_{WZ/ZZ}$ marginalized over nuisance parameters, is shown after projection on the σ_{WW} (left) and $\sigma_{WZ/ZZ}$ (right) axes. The measured cross sections correspond to the maximum value of the projected posterior: $\sigma_{WW}^{Obs} = 0.45^{+0.35}_{-0.32} \times \sigma_{WW}^{SM}$ and $\sigma_{WZ/ZZ}^{Obs} = 1.64^{+0.83}_{-0.78} \times \sigma_{WZ/ZZ}^{SM}$. The blue and azure areas represent the smallest intervals enclosing 68% and 95% of posterior integrals, respectively.

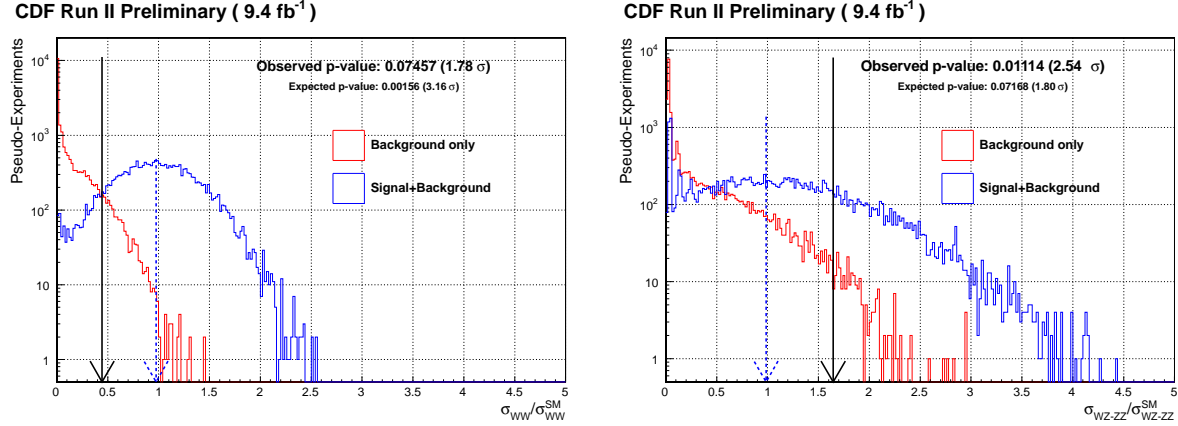


Figure 9: Possible outcomes of many diboson cross section measurements on Pseudo Experiments (PEs) generated in a background-only and in a background+signal hypothesis in the σ_{WW} vs $\sigma_{WZ/ZZ}$ plane and then projected on the σ_{WW} (left) and $\sigma_{WZ/ZZ}$ (axis). The p-values of 0.074565 and 0.011145 correspond to a significance of 1.78 σ and 2.54 σ for WW and WZ/ZZ respectively.

al., Nucl. Instrum. Methods Phys. Res. A **350**, 73 (1994); F. Abe, et al., Phys. Rev. D **52**, 4784 (1995); P. Azzi, et al., Nucl. Instrum. Methods Phys. Res. A **360**, 137 (1995); The CDF II Detector Technical Design Report, Fermilab-Pub-96/390-E

- [4] A.Bhatti et al., Nucl. Instrum. Methods, **A566**, 2 (2006).
- [5] D. Acosta, et al., Phys. Rev. D **71**, 052003 (2005).
- [6] G. Chiarelli, V. Lippi, F. Sforza, “Rejection of multi-jet background in $p\bar{p} \rightarrow e\nu + jj$ channel through a SVM classifier”, J. Phys.: Conf. Ser. **331** 032045 (2011).
- [7] Chang C. C. and Lin C. J. 2001 ”LIBSVM: a library for support vector machines”.
- [8] M.L. Mangano et al, JHEP 0307:001,2003, hep-ph/0206293.
- [9] T. Aaltonen et al. (CDF Collaboration), Phys. Rev. D **82**, 112005 (2010).
- [10] T. Aaltonen et al. (CDF Collaboration), Fermilab-Pub-11-664-E, Accepted by PRD, arXiv:1112.4358.
- [11] T Sjostrand et al., T. Sjostrand et al., High-Energy-Physics Event Generation with PYTHIA 6.1, Comput. Phys. Commun. **135**, 238 (2001).
- [12] T. Junk, “Sensitivity, Exclusion and Discovery with Small Signals, Large Backgrounds, and Large Systematic Uncertainties”, CDF Public Note 8128 (2007).
- [13] T. Aaltonen et al., “Search for Standard Model Higgs Boson Production in Association with a W Boson using Neural Networks with 9.45fb-1 of CDF Data”, CDF Public Note 10796 (2011).